BIOCHEMISTRY
including biophysical chemistry & molecular biology

Article

pubs.acs.org/biochemistry

Inhibitory Mechanism of Pancreatic Amyloid Fibril Formation: Formation of the Complex between Tea Catechins and the Fragment of Residues 22−27

Miya Kamihira-Ishijima,[†] Hiromi Nakazawa,[†] Atsushi Kira,[‡] Akira Naito,[§] and Tsutomu Nakayama*[,†]

[†]Laboratory of Molecular Food Engineering and Global COE Program, School of Food and Nutritional Sciences, University of Shizuoka, 52-1 Yada, Suruga-ku, Shizuoka 422-8526, Japan

[‡]Research and Development Division, ULVAC, Inc., 2500 Hagizono, Chigasaki, Kanagawa 253-8543, Japan

[§]Faculty of Engineering, Yokohama National University, 79-5 Tokiwadai, Hodogaya-ku, Yokohama 240-8501, Japan

Supporting Information

ABSTRACT: Islet amyloid polypeptide (IAPP) is a major component of pancreatic amyloid deposits associated with type 2 diabetes. Polyphenols contained in plant foods have been found to inhibit amyloid fibril formation of proteins and/or peptides. However, the inhibition mechanism is not clear for a variety of systems. Here the inhibition mechanism of green tea polyphenols, catechins, on amyloid fibril formation of the IAPP fragment (IAPP22−27), which is of sufficient length for formation of β-sheet-containing amyloid fibrils, was investigated by means of kinetic analysis. A quartz crystal microbalance (QCM) determined that the association constants of gallate-type catechins [epicatechin 3-gallate (ECg) and epigallocatechin 3-gallate] for binding to IAPP22−27 immobilized on the gold plate in QCM were 1 order of magnitude larger than those of the free IAPP22−27 peptide, and also those of epicatechin and epigallocatechin. Kinetic analysis using a two-step autocatalytic reaction mechanism revealed that ECg significantly reduced the rate constants of the first nucleation step of amyloid fibril formation, while the rate of autocatalytic growth was less retarded. ^{1}H nuclear magnetic resonance studies clarified that a IAPP22−27/ECg complex clearly forms as viewed from the ^{1}H chemical shift changes and line broadening. Our study suggests that tea catechins specifically inhibit the early stages of amyloid fibril formation to form amyloid nuclei by interacting with the unstructured peptide and that this inhibition mechanism is of great therapeutic value because stabilization of the native state could delay the pathogenesis of amyloid diseases and also the toxicity of the small oligomer (protofibril) is reported to be greater than that of the mature fibril.

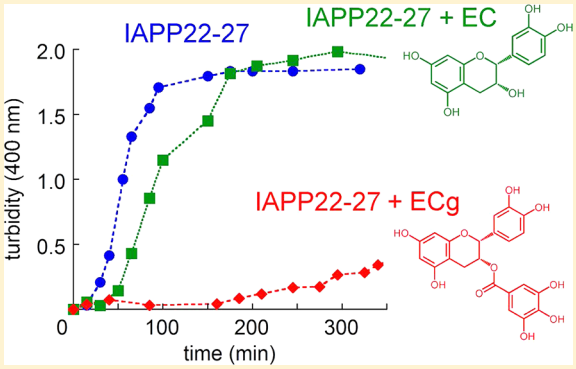

Amyloid fibril formation is well-known as the common phenomenon associated with severe diseases such as Alzheimer's, Parkinson's, and Creutzfeld-Jakob diseases.[1,2] Although the sequence of the proteins and/or peptides forming the amyloid fibrils is different, the fibrils show common morphology such as 80−150 nm in diameter,[3] specific characteristics such as the appearance of apple green birefringence in aggregates stained with Congo red,[4] and increased intensity of fluorescence by thioflavin T.[5] The assembly of amyloid fibrils is accompanied by conformational changes in the proteins and/or peptides, and the resulting fibrils mainly form β-sheet structures.[6] Because elucidation of the molecular mechanism of fibril formation is important for preventing and/or delaying the outbreak of such diseases, many studies have been conducted. Plausible forces for the assembly of proteins and/or peptides are generally considered to be hydrophobic and charge−charge interactions between the side chains. Fibrillation mechanisms have been proposed, and in most cases, the nucleus of the fibril is formed during the early stage. During the nucleation phase, no detectable amyloid fibrils are formed, and therefore, a lag phase is displayed. It is followed by more rapid growth, an elongation phase that leads to a final state in which amyloid fibrils are in equilibrium with soluble peptides. As a simple, relevant model, a two-step autocatalytic reaction mechanism was proposed for the case of amyloid fibril formation of human calcitonin (hCT), where the first step is the nucleation process and the second step is the elongation process.[7−9] Once the nucleus of the fibril is formed, the reaction is accelerated by an autocatalytic reaction. Prevention of the association process of peptides and/or proteins at the onset to form nuclei is one of the particular challenges to delay the development of severe symptoms.[10] A higher neurotoxicity of small oligomers or protofibrils as compared with that of

Received: September 10, 2012
Revised: December 2, 2012
Published: December 3, 2012

mature fibrils was seen for amyloid aggregates by Alzheimer's β-amyloid (Aβ).[11]

Human islet amyloid polypeptide (IAPP, amylin) consists of 37 amino acid residues and contains the sequence KCNTATCAT QRLANFLVHS SNNFGAILSS TNVGSNTY-NH_2 with a disulfide bond between Cys^2 and Cys^7. It is one of the amyloid-forming peptides observed in extracellular pancreatic deposits in type 2 diabetes; this aggregate is found to be strongly toxic to pancreatic β-cells.[12] Pancreatic amyloid deposition is not found in rodents, although there are only six amino acid residues by which the rat IAPP differs from that of humans; five of the six amino acid residues are located in the region between residues 20 and 29.[13] In particular, substitution of the fragment of residues 20−29 with one or two amino acid residues with Pro or another amino acid generally weakened the ability to form fibrils.[13,14] Fragments 23−27 and 22−27 of IAPP were shown to be of sufficient length for formation of amyloid fibril with a β-sheet conformation.[15]

Inhibition of amyloid fibril formation by peptides and small compounds has been examined in vivo and in vitro.[16−21] Polyphenols have demonstrated an inhibitory effect on amyloid fibril formation. This phenomenon was mostly attributed to the antioxidative nature of these compounds, although it also has been suggested that structural properties of polyphenol compounds may affect their inhibitory nature.[21] Experimental and theoretical studies suggest that aromatic interactions play an important role in many cases of amyloid protein self-assembly by affecting the directionality and orientation needed for this process.[8,22−24] Tea catechins, polyphenols in green teas, are known to have a variety of biological activities such as antioxidant,[25] antimicrobial,[26] and antitumor activities.[27] In tea leaves, the major catechins are (−)-epicatechin (EC), (−)-epicatechin 3-gallate (ECg), (−)-epigallocatechin (EGC), (−)-epigallocatechin 3-gallate (EGCg), (−)-gallocatechin (GC), and (+)-catechin (C). In vitro work has shown that C inhibits Aβ aggregation,[28] and EGCg inhibits amyloid formation of Aβ, α-synuclein, polyglutamine peptides, the model polypeptide κ-casein, hCT, and also IAPP.[29−33] However, the detailed inhibition mechanism is not yet clear.

Here, we aim to investigate the effect of catechins on amyloid fibril formation of IAPP22−27 [NFGAIL (see the underlined part of the hIAPP sequence)] peptide by evaluating quantitative kinetic rate constants. This fragment was chosen because the region was shown to play a central role in amyloid fibril formation of IAPP.[15] Although the sequence is simple, it contains aromatic and hydrophobic amino acids that could plausibly play important roles in the molecular assembly of amyloid fibrils. Four tea catechins (Figure 1) were applied to the IAPP22−27 peptide as possible inhibitors. To investigate peptide−peptide and peptide−catechin interactions, we used a quartz crystal microbalance (QCM). In previous studies, a 27 MHz QCM was successfully employed to quantitatively analyze interactions by tracking mass changes between transcription proteins and/or peptides and DNA[34,35] or substrate−enzyme reactions[36,37] in aqueous solution. The interaction of bioactive compounds and a lipid-coated QCM was also investigated.[38−40] The association constants (K_a) for peptide−peptide and peptide−catechin interactions were calculated by experimentally obtained association rate constants (k_{on}) and dissociation rate constants (k_{off}). The kinetics of insoluble IAPP22−27 fibril formation was studied in the absence and presence of catechins by turbidity measurements and analyzed using the two-step reaction mechanism. Consequently, the rate constants for nucleation (k_1) and autocatalytic elongation (k_2) were determined quantitatively. Nuclear magnetic resonance (NMR) spectroscopy was applied to examine the peptide−catechin interaction at the molecular level.

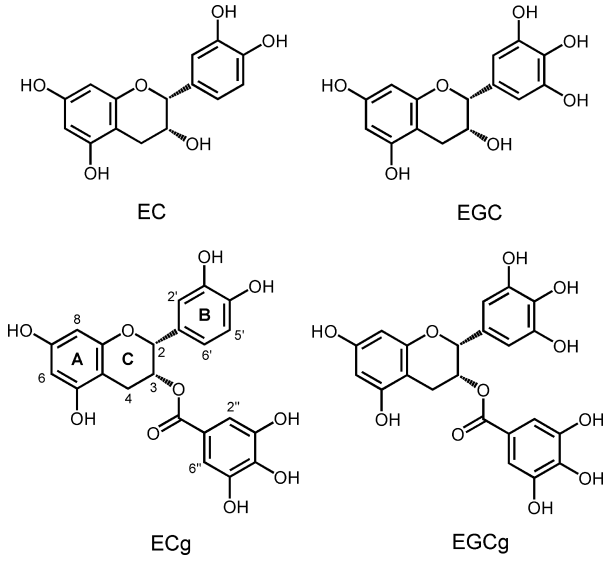

Figure 1. Structures of tea catechins: (−)-epicatechin (EC), (−)-epigallocatechin (EGC), (−) epicatechin 3-gallate (ECg), and (−)-epigallocatechin 3-gallate (EGCg).

EXPERIMENTAL PROCEDURES

Materials. Lyophilized IAPP22−27 peptide was obtained from custom peptide synthesis services by Invitrogen Co. (Tokyo, Japan) at >95% purity. Tea catechins, EC, EGC, ECg, and EGCg, were kindly provided by Mitsui Norin Co. The other chemicals were purchased from Sigma-Aldrich Japan and used without further purification.

QCM Experiment. A 27 MHz QCM (Affinix Q4, Initium Inc., Tokyo, Japan) was used for QCM measurements. It is characterized by four channels for simultaneous measurements of 500 μL cells equipped with an AT-cut quartz crystal plate and a gold electrode with an area of 4.9×10^{-6} m^2 at the bottom of the cell, a stirring bar, and a temperature controlling system (Initium Inc.). IAPP22−27 peptide was covalently immobilized on the gold surface, in accordance with a previously published method.[41] Phosphate-buffered saline {PBS [1/15M, 137 mM NaCl, and 2.7 mM KCl (pH 7.4)]} containing 1 mM peptide was kept in the cell for 60 min and was adopted as the binding condition. For experiments, an IAPP22−27 peptide or catechin solution dissolved in PBS was injected into the cells as a guest molecule. Because DMSO is not suitable for the QCM system, the peptide was dissolved in PBS and stocked in the freezer (−20 °C) until injection. No fibril formation was observed in the QCM cell during measurement because the concentration of IAPP22−27 in the cell was kept below thermodynamic solubility (1.2 ± 0.2 mg/mL, 1.9 mM).[15] All measurements were taken at 25 °C.

Sauerbrey's equation (eq 1) was applied to calculate the mass of the adsorbed molecules.

$$\Delta F = -\frac{2F_0^2}{A\sqrt{\mu_q \rho_q}}\Delta m \quad (1)$$

dx.doi.org/10.1021/bi3012274 | Biochemistry 2012, 51, 10167−10174

where ΔF is the change in frequency, F_0 is the fundamental frequency of QCM (27×10^6 Hz), A is the electrode area (4.9×10^{-6} m^2), μ_q is the shear mode stress of the crystal (2.95×10^{10} kg m^{-1} s^{-2}), ρ_q is the density of the quartz (2648 kg/m^3), and Δm is the mass change (grams). As a result, a frequency decrease of 1 Hz corresponds to 30 pg binding to the electrode.

The process of binding of free IAPP22−27 or catechins to the immobilized IAPP22−27 on the gold plate in QCM is assumed to be in the equilibrium given by eq 2.

$$X + Y \underset{k_{off}}{\overset{k_{on}}{\rightleftarrows}} X{\cdot}Y \tag{2}$$

where X is the IAPP22−27 peptide immobilized on the gold surface and Y is a guest molecule injected later. K_a is obtained from the ratio of k_{on} to k_{off}. The amount of the X·Y complex after a certain time t from the injection is given by eq 3

$$\Delta m_t = [X{\cdot}Y] = [X{\cdot}Y]_{max}\left[1 - \exp\left(\frac{-t}{\tau}\right)\right] \tag{3}$$

where

$$\frac{1}{\tau} = k_{on}[Y] + k_{off} \tag{4}$$

From the linear correlation of $1/\tau$ and [Y], k_{on} and k_{off} values could be obtained from the slope and intercept, respectively.

Kinetic Analysis of Fibrillation. EGCg is an abundant catechin in tea extract and is known to demonstrate various biological activities. However, it was found to be unstable especially in a neutral pH solution because the gallyl moiety in the B-ring of gallocatechins EGC and EGCg contributed to H_2O_2 formation.[42,43] Therefore, ECg and EC were used in this kinetic research after their stability had been confirmed.

The kinetic fibrillation assay of IAPP22−27 was performed using a UV−vis spectrometer (U-3300, Hitachi, Tokyo, Japan). The peptide stock solution was prepared by dissolving the lyophilized powder completely in DMSO at a concentration of ~120 mM by immediate mixing and sonication and used immediately to avoid formation of preaggregated peptide seeds.[15,44] The fibrillation assay was initiated by adding pH 6.8 buffer (50 mM phosphate buffer and 100 mM NaCl). The final peptide concentration (2.3−2.5 mM) was estimated from the added mass of peptide powder, and the final DMSO content of the test solution was 4%. The solutions were continuously stirred with a magnetic stirring bar (2 mm × 2 mm) in a disposable cuvette (path length of 1 cm) at room temperature (20−22 °C), and turbidity (absorbance at 400 nm) was measured over several time points. An IAPP22−27 solution in the presence of catechin was prepared by adding ECg or EC dissolved in DMSO and diluted into the phosphate buffer to the peptide stock solution. Fibrillation assays with or without catechins were always performed in duplicate in the same experimental set, and measurements were repeated in three independent experiments. Stirring is well-known to increase the rate of amyloid formation and generates small fibrils that would exhibit turbidity.[45] Fibrillation assays presented here were all performed under the same stirring conditions, which yielded good reproducibility.

A two-step reaction mechanism was adopted for the analysis of amyloid fibril formation of hCT[7−9] and used for that of IAPP22−27: the first reaction step is a homogeneous association to form fibril nucleus, and the second step is an autocatalytic heterogeneous fibrillation to allow the fibril to mature. The rate constants for the first (k_1) and second (k_2) steps were analyzed using the following equation.

$$f = \frac{\rho\{\exp[(1+\rho)kt] - 1\}}{1 + \rho\{\exp[(1+\rho)kt]\}} \tag{5}$$

where f is the fraction of fibril form in the total peptide molecules (a dimensionless value), $\rho = k_1/k$, $k = ak_2$, and the initial peptide concentration is represented as a.

NMR Observation. ^{1}H NMR experiments were performed on a Bruker Avance III spectrometer operating at the proton resonance frequency of 500.13 MHz. IAPP22−27 was dissolved in DMSO-d_6. Then 50 mM phosphate buffer [100 mM NaCl (pH 6.8)] was added. Samples in the presence of catechins were prepared by dissolving catechins in DMSO-d_6 and mixed with lyophilized IAPP22−27 powder, and then the pH 6.8 buffer was added to reach a 10:1 molar ratio of catechin to peptide. The final peptide concentration was 2.9−3.4 mM, and 10% DMSO-d_6 was necessary to dissolve catechins completely. The apparent pH value for the samples was 6.0. The proton chemical shift value was referred to that of internal sodium 3-(trimethylsilyl)propionate-2,2,3,3-d_4 (TSP-d_4) at 0 ppm. The residual water resonance was suppressed using a Watergate sequence. Signal assignments of the peptide and catechins were taken by TOCSY and NOESY measurements. NMR spectra were recorded at 20 ± 2 °C.

RESULTS AND DISCUSSION

IAPP22−27−Catechin Interaction Revealed by QCM. The interaction between IAPP22−27 immobilized on the gold plate in the 27 MHz QCM (IAPP-QCM) and free IAPP22−27 (IAPP-F) in solution was investigated. Figure 2A shows typical

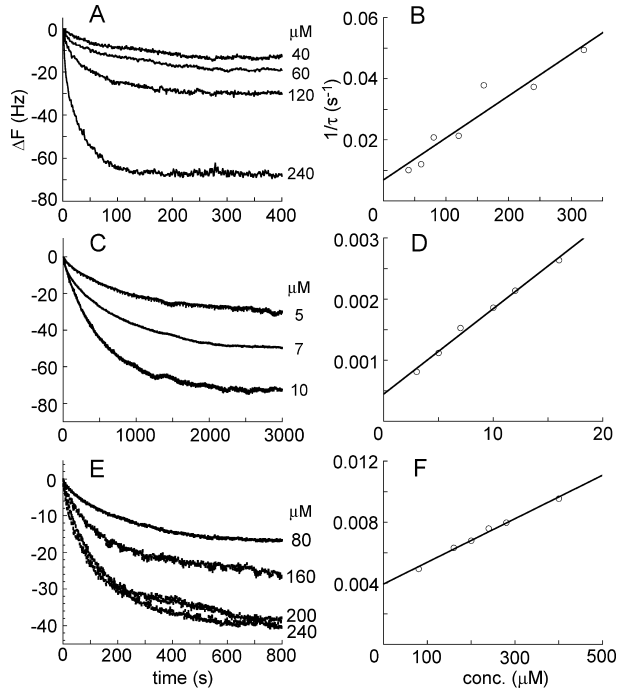

Figure 2. Typical time courses of changes in frequency for the IAPP22−27 immobilized in the QCM (A, C, and E) and linear reciprocal plots of relaxation rate ($1/\tau$) vs IAPP22−27 concentration according to eq 3 in the text (B, D, and F), in response to the addition of IAPP22−27 (A, B), ECg (C, D), and IAPP22−27 after ECg was reacted in advance (PBS, pH 7.4, 25 °C) (E, F).

dx.doi.org/10.1021/bi3012274 | Biochemistry 2012, 51, 10167−10174

time courses of changes in frequencies. The decrease in frequency observed corresponded to the amount of IAPP-F that interacted with IAPP-QCM. The value of $1/\tau$ for each peptide concentration was determined by fitting the curves in Figure 2A using eq 3, and k_{on} and k_{off} were obtained (Figure 2B). Table 1 summarizes the k_{on} and k_{off} values together with K_a.

Table 1. Kinetic Parameters of IAPP22−27 (IAPP-F) and Catechins during the Interaction with IAPP22−27 on the QCM Plate (IAPP-QCM)

	k_{on} (M^{-1} s^{-1})	k_{off} ($\times 10^{-3}$ s^{-1})	K_a ($\times 10^4$ M^{-1})[a]
IAPP22−27	138 ± 19	6.94 ± 3.34	1.98 ± 1.00
EC	19.4 ± 12.7	0.613 ± 0.062	4.85 ± 0.38
EGC	16.8 ± 1.7	0.829 ± 0.107	2.03 ± 0.33
ECg	140 ± 6	0.449 ± 0.060	31.1 ± 4.4
EGCg	252 ± 7	1.65 ± 0.09	15.3 ± 0.9
IAPP22−27 with ECg	14.2 ± 0.6	3.97 ± 0.15	0.359 ± 0.021

[a]Calculated from $K_a = k_{on}/k_{off}$.

Addition of catechin solutions to the IAPP-QCM also displayed significant changes in frequencies. Figure 2C shows typical changes in frequencies caused by the interaction between injected ECg and IAPP-QCM, and Figure S1 of the Supporting Information shows those between EC, EGC, and EGCg and IAPP-QCM. The observed frequency changes indicate the interaction of catechins with IAPP-QCM; the frequency decreases upon the addition of ECg and EGCg were, however, larger than those upon the addition of EC and EGC. Table 1 summarizes k_{on}, k_{off}, and K_a values for the interaction between catechins and IAPP-QCM. It was revealed that the order of the k_{on} values was as follows: EGCg > ECg > EC > EGC. The order of the k_{off} values was as follows: EGCg > EGC > EC > ECg. The order of the resulting K_a values was as follows: ECg > EGCg > EC > EGC. It should be mentioned that the k_{off} values for the four catechins against IAPP-QCM were smaller than that for IAPP-F, and consequently, K_a values for ECg and EGCg especially were significantly larger than that for free IAPP22−27 (Table 1). These findings demonstrate that ECg and EGCg in particular could be strong inhibitors for the peptide−peptide interactions compared with EC and EGC. Namely, the galloyl group in the catechin structure plays an important role in association with the peptide, whereby the order is concomitantly consistent with hydrophobicity.[46] The relatively large dissociation rate constant obtained for EGCg might be due to its large steric hindrance upon interaction with IAPP-QCM.

To examine whether ECg directly disturbs the peptide−peptide interaction, ECg was reacted first with the IAPP-QCM and then IAPP-F was injected (Figure 2E). Frequency decreases shown in Figure 2E were significantly reduced compared with those without ECg (Figure 2A). k_{on} and K_a values were determined to be 1 order of magnitude smaller than those without ECg (Table 1). We conclude that ECg strongly prevents the interaction between the IAPP-F peptide and the IAPP-QCM peptide.

Inhibitory Effects of Catechins on IAPP22−27 Revealed by Fibrillation Kinetics. To evaluate the inhibitory effect of ECg on IAPP22−27 fibril formation, the fibrillation of IAPP22−27 was compared with that in the presence of EC or ECg. To verify the specificity of ECg toward IAPP22−27, EC, in which the galloyl group is lacking, was used as a control. The fibrillation assays were performed at pH 6.8 to avoid the base-catalyzed degradation of EC and ECg (see Figure S2 of the Supporting Information).

The IAPP22−27 peptide in aqueous solution [2.35 ± 0.04 mM in 5 mM phosphate buffer, 0.1 M NaCl, and 4% DMSO (pH 6.8)] started forming white fluffy lumps after a 20−30 min lag time from dissociation under stirring, which was observed by turbidity at 400 nm (Figure 3A,B). Turbidity increased

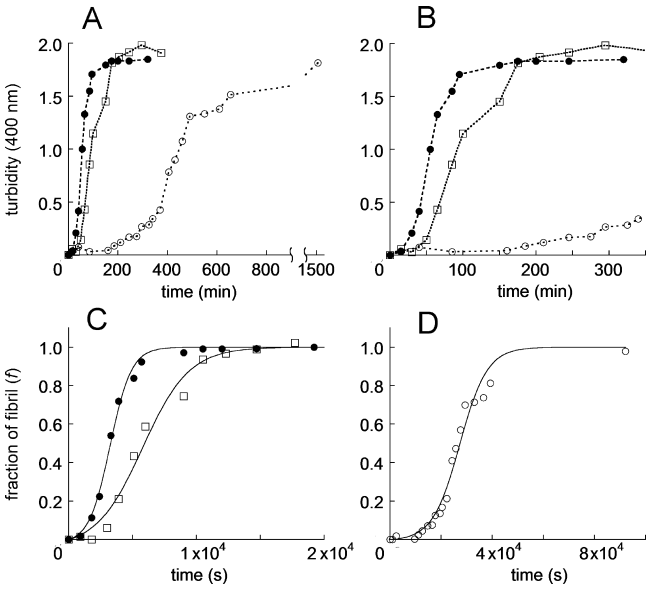

Figure 3. (A) Typical time courses of turbidity changes (400 nm) accompanied by IAPP22−27 amyloid fibril formation in the absence and presence of EC and ECg: (●) IAPP22−27 alone, (□) a 1:1 molar ratio mixture of IAPP22−27 and EC, and (○) a 1:1 molar ratio mixture of IAPP22−27 and ECg. An expansion of panel A is shown in panel B. The peptide concentration was 2.40−2.43 mM in 50 mM phosphate buffer, 100 mM NaCl, and 4% DMSO (pH 6.8), and the measurements were taken at 20−22 °C. (C and D) The absorbance was normalized by setting the maximal absorbance to 1 to demonstrate the fraction of fibril in the system. The turbidities 320 min [IAPP22−27 alone (●, C)], 375 min [a 1:1 molar ratio mixture of IAPP22−27 and EC (□, C)], and 1535 min [a 1:1 molar ratio mixture of IAPP22−27 and ECg (○, D)] after dissolution were used for the maximal absorbance. Solid lines are calculated using eq 5 to show the best fits to the experimentally obtained values.

gradually and reached a plateau after ∼200 min. It was fractionalized by setting the maximal value to 1 to fit with the autocatalytic reaction mechanism (eq 5) to obtain the reaction rate constants k_1 and k_2 (Figure 3C). Table 2 summarizes the rate constants.

In the presence of catechins (EC and ECg), fibrillation of the IAPP22−27 peptide in the solution was observed. However, at a 1:1 molar ratio of IAPP22−27 to ECg, the lag time for peptide fibrillation was remarkably lengthened, and increases in turbidity began after ∼200 min from dissociation (Figure 3A,B). Turbidity increased slowly and reached equilibrium after 1 day. The reaction rate constants, k_1 and k_2, of IAPP22−27 fibrillation in the presence of ECg were obtained (Figure 3D and Table 2). It was clearly shown that the addition of ECg reduced the k_1 of IAPP22−27 fibril formation by approximately 300-fold, and k_2 was also ∼3 times slower than that without ECg (Table 2).

Addition of EC at a 1:1 molar ratio with IAPP22−27 delayed the lag time of IAPP22−27 fibril formation slightly (∼40 min)

dx.doi.org/10.1021/bi3012274 | Biochemistry 2012, 51, 10167−10174

Table 2. Kinetic Parameters of IAPP22−27 Fibril Formation

	a ($\times 10^{-3}$ M)[a]	k_1 ($\times 10^{-5}$ s^{-1})	k_2 ($\times 10^{-1}$ s^{-1} M^{-1})	ak_2 ($\times 10^{-4}$ s^{-1})
IAPP22−27	2.35 ± 0.02	9.24 ± 6.27	3.39 ± 1.04	8.02 ± 2.50
IAPP22−27 with EC[b]	2.40 ± 0.03	2.20 ± 0.02	3.26 ± 1.09	7.80 ± 2.51
IAPP22−27 with ECg[b]	2.46 ± 0.03	0.028 ± 0.013	1.07 ± 0.05	2.62 ± 0.11

[a]Initial peptide concentration. [b]The concentrations of EC and ECg were 2.41 ± 0.04 and 2.46 ± 0.03 mM, respectively.

(Figure 3B). The resultant k_1 of IAPP22−27 fibrillation was ∼4 times lower than that in the absence of EC, and k_2 was not modified (Table 2). It clearly demonstrated that ECg and EC inhibit IAPP22−27 fibrillation on the first nucleation step; furthermore, ECg more effectively inhibits fibrillation than EC does.

The first nucleation step is considered to be the peptide−peptide association to lead to conformational changes to β-sheet structures as nuclei of the amyloid fibrils.[7] It was in good agreement with the QCM analysis that EC and ECg exhibit larger association constants for the IAPP22−27 peptide than the peptide−peptide interaction itself. Accordingly, the catechin−peptide interaction would disturb the association of peptides to form fibril nuclei. Generally, amyloid fibril formation is efficiently accelerated by seeding its preaggregated species. However, recent studies demonstrated that as seeds, EGCg-associated Aβ, α-synuclein, and full length IAPP oligomers did not catalyze amyloid fibril formation by the parent peptide or protein.[29,32] The authors of those studies suggested that EGCg may have trapped the respective polypeptides in an early intermediate state that had not yet reached the state where it is capable of promoting growth of cross-β-structure. The results obtained here are in good agreement with their findings.

The second step in the autocatalytic reaction mechanism is the elongation process of amyloid fibrils by the association of soluble peptides with the nuclei and/or protofibrils formed in the first step. It is suggested that ECg or EC preferably interacts with soluble, unstructured IAPP22−27 peptides rather than the peptides in β-sheet form. Generally, formation of an ordered nucleus is the rate-determining step of fibril formation, while that of elongation of the amyloid fibril on the nucleus is the rapid assembly of the peptides. In the presence of ECg, the interaction between ECg and soluble IAPP22−27 peptides might have delayed the rapid elongation process as well. In fact, preliminary transmission electron microscope observations showed that the length of mature IAPP22−27 amyloid fibrils in the presence of ECg was shorter than when ECg was absent (Figure S3 of the Supporting Information). It is therefore concluded that the reaction rate of the second growth step was not much influenced by the catechins, but ECg might also act to disturb the elongation of the IAPP22−27 amyloid fibrils by interacting with soluble IAPP22−27 peptides.

Sites of Interaction of Catechin with IAPP22−27 Revealed by NMR Measurements. ^{1}H NMR spectra of IAPP22−27 alone or with a 1:10 molar ratio with EC or ECg was measured. Amide and sometimes α-proton signals of Phe in the IAPP22−27 peptide were not observed. This may be due to suppression of the signal of the α-proton of Phe because it is close to that of water.

All the α-protons and amide protons of IAPP22−27 shifted downfield in the presence of a 10-fold excess of ECg, whereas they merely shifted when a 10-fold excess of EC was added to the peptide solution (Figures 4 and 5A). Upon interaction with ECg, the ^{1}H resonances of the peptide side chains also shifted

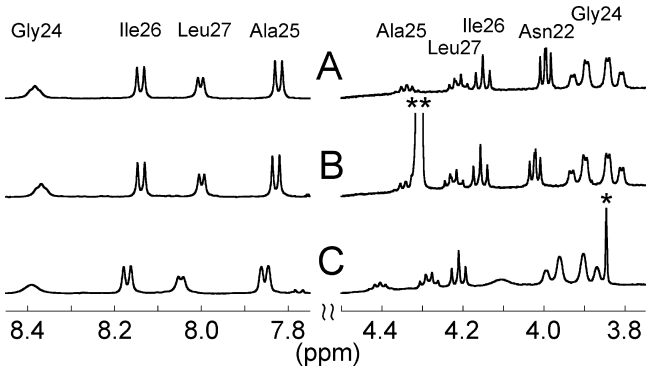

Figure 4. ^{1}H NMR spectra of IAPP22−27 (A), a 1:10 molar ratio mixture of IAPP22−27 and EC (B), and a 1:10 molar ratio mixture of IAPP22−27 and ECg (C) [50 mM phosphate buffer, 100 mM NaCl, and 10% DMSO (pH 6.8)]. Resonances of the amide (left column) and α-proton (right column) region are shown. One asterisk and two asterisks show a small amount of impurity and a signal of EC (3-H), respectively.

downfield, while only those of Phe shifted upfield slightly (Figure 5B). Addition of a 10-fold excess of EC to the peptide did not change the proton resonances of the peptide side chains significantly (Figure 5B).

Figure 6 shows ^{1}H NMR signals of B-rings (see Figure 1) and galloyl rings of catechins in the absence and presence of the IAPP22−27 peptide. For EC, resonances when bound with the peptide did not shift significantly, but the extent of signal splitting by the interaction obviously increased (Figure 6A,B). In contrast, ^{1}H chemical shifts of ECg resonances changed upon reaction: only 6′-H signals of ECg shifted upfield, whereas 2′-, 5′-, and 2″,6″-H signals shifted downfield (Figures 5C and 6C,D). The signals of ECg in the presence of IAPP22−27 were broadened compared with those of free ECg (Figure 6C,D). Accompanied by the signal changes, 2-H signals of EC and ECg shifted extensively in the presence of the peptide (Figure 5C). In the case of ECg, 6-H/8-H signals also shifted downfield upon interaction with IAPP22−27.

Chemical shift changes and line widths of the NMR signals clearly demonstrate the formation of a peptide/catechin complex in the case of ECg, and ECg is a more effective inhibitor of formation of fibrils by the IAPP22−27 peptide than EC. As was shown by the QCM and fibrillation kinetic results described above, it was revealed that the galloyl moiety plays an important role in the interaction with the IAPP22−27 peptide. Indeed, the 2″,6″-H signal of ECg shifted during the interaction (Figures 5C and 6D). The IAPP22−27 peptide contains hydrophobic side chains at the C-terminal side. Upon binding with ECg, the galloyl moiety of ECg might be close to the hydrophobic rich area of the peptide. It is of interest to notice that during the interaction with EC or ECg, the resonances of the Phe ring in the peptide shifted upfield slightly while the other signals shifted downfield (Figure 5B). The possible $\pi-\pi$ interaction, if any, between the Phe ring and phenol rings in the

dx.doi.org/10.1021/bi3012274 | Biochemistry 2012, 51, 10167−10174

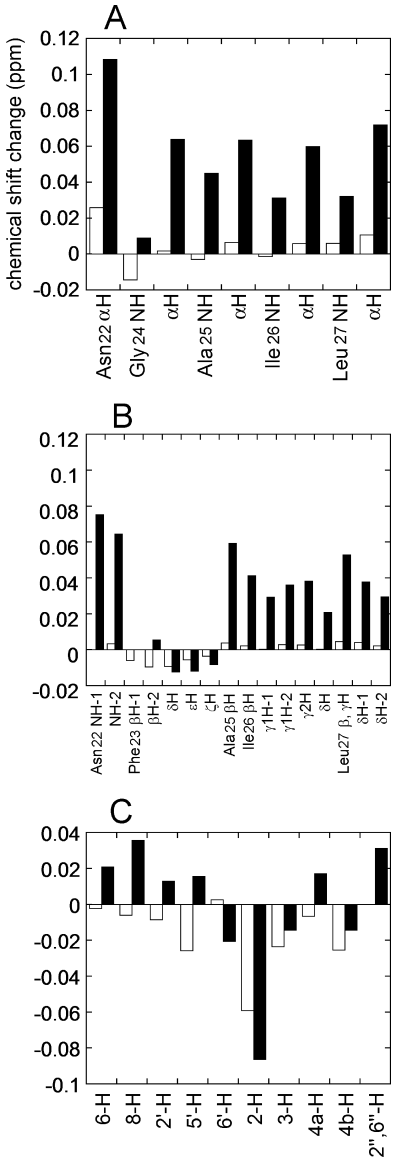

Figure 5. ^{1}H chemical shift deviation of peptide backbone (A) and side chain (B) signals of IAPP22−27 and catechin signals (C) upon interaction with a 10-fold molar excess of EC (white bars) and ECg (black bars) with IAPP22−27.

catechins could cause the ring current effect that may alter the chemical shift direction. The B-ring of EC and ECg may also be important for the association with the IAPP22−27 peptide, because the 2-H signal of EC and ECg shifted most significantly (Figure 5C). Hydrogen bonding to the peptide via phenolic hydroxyl groups of catechins may also contribute to stabilization of the peptide/catechin complex. It should also be mentioned that the ECg solution in the presence of the IAPP22−27 peptide did not change color, nor were additional NMR signals found even after 2 weeks (data not shown). By the formation of the peptide/ECg complex, the structure of ECg may be protected from degradation.

CONCLUSIONS

Kinetic rate constants obtained by QCM measurements clarified that tea catechins, especially ECg and EGCg, have the ability to inhibit the formation of amyloid fibrils by IAPP22−27 by disturbing the peptide−peptide association.

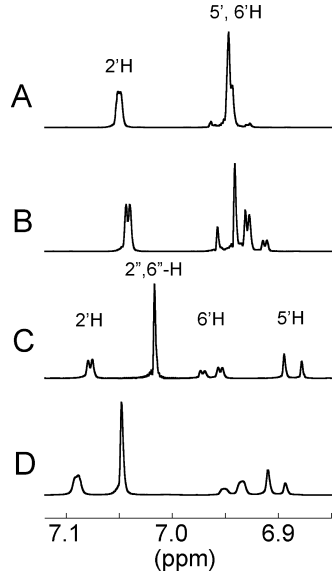

Figure 6. ^{1}H NMR spectra of EC alone (A), a 1:10 molar ratio mixture of IAPP22−27 and EC (B), ECg alone (C), and a 1:10 molar ratio mixture of IAPP22−27 and ECg (D). The proton signals of C-rings and galloyl rings of catechins are shown.

The formation of insoluble fibrils by IAPP22−27 was evaluated by turbidity measurements, and increases in turbidity showed that fibril formation follows a two-step autocatalytic reaction mechanism. In the presence of ECg, the rate of the first nucleation step of formation of fibrils by IAPP22−27 was significantly decreased, while the second growth step was retarded slightly. EC delayed the nucleation step; however, the effect was much smaller than that of ECg. Association between IAPP22−27 and ECg was demonstrated by ^{1}H NMR chemical shift changes and increased line widths. This study demonstrated that the hydrophobic galloyl moiety in the structure of catechins plays an important role in the interaction with the IAPP22−27 amyloid-forming peptide. It is believed that inhibition of the early stages of amyloid fibril formation is of great therapeutic value,[10] specifically before the nucleus of the amyloid fibril is formed. This study showed that food component catechins could be desirable inhibitors for preventing the risks of disease.

ASSOCIATED CONTENT

Supporting Information

Frequency changes of the IAPP22−27-immobilized QCM in response to the addition of EC, EGC, and EGCg (Figure S1), typical time course of absorbance changes at 400 nm for catechin solutions (EC and ECg) (Figure S2), and TEM images of IAPP22−27 fibrils with and without EC and ECg (Figure S3). This material is available free of charge via the Internet at http://pubs.acs.org.

AUTHOR INFORMATION

Corresponding Author

*Telephone: +81-54-264-5522. Fax: +81-54-264-5551. E-mail: nkymttm@u-shizuoka-ken.ac.jp.

Funding

Grants-in-Aid for Scientific Research from the Ministry of Education, Science, Sports and Culture of Japan (18780101) to M.K.-I. and Shizuoka Prefecture Collaboration of Regional

Entities for the Advancement of Technological Excellence, JST, to T.N.

Notes

The authors declare no competing financial interest.

■ ACKNOWLEDGMENTS

We thank Mr. Masao Kondo of the Instrumental Analysis Center of Yokohama National University for his help with TEM measurements. We also thank Professor Kazue Kurihara at Tohoku University (Sendai, Japan) for use of UV−vis and NMR spectrometers.

■ ABBREVIATIONS

IAPP, islet amyloid polypeptide; QCM, quartz crystal microbalance; EC, (−)-epicatechin; ECg, (−)-epicatechin 3-gallate; EGC, (−)-epigallocatechin; EGCg, (−)-epigallocatechin 3-gallate; GC, (−)-gallocatechin; C, (+)-catechin; Aβ, Alzheimer's β-amyloid; hCT, human calcitonin; DMSO, dimethyl sulfoxide; PBS, phosphate-buffered saline; TSP, sodium 3-(trimethylsilyl)propionate-2,2,3,3; IAPP-QCM, IAPP22−27 immobilized on the gold plate in the 27 MHz QCM; IAPP-F, free IAPP22−27.

■ REFERENCES

(1) Sipe, J. D. (1994) Amyloidosis. *Crit. Rev. Clin. Lab. Sci. 31*, 325−354.

(2) Taylor, J. P., Hardy, J., and Fischbeck, K. H. (2002) Toxic proteins in neurodegenerative disease. *Science 296*, 1991−1995.

(3) Dobson, C. M. (2003) Protein folding and misfolding. *Nature 426*, 884−890.

(4) Westermark, G. T., Johnson, K. H., and Westermark, P. (1999) Staining methods for identification of amyloid in tissue. *Methods Enzymol. 309*, 3−25.

(5) LeVine, H. (1999) Quantification of β-sheet amyloid fibril structures with thioflavin T. *Methods Enzymol. 309*, 274−284.

(6) Rochet, J. C., and Lansbury, P. T., Jr. (2000) Amyloid fibrillogenesis: Themes and variations. *Curr. Opin. Struct. Biol. 10*, 60−68.

(7) Kamihira, M., Naito, A., Tuzi, S., Nosaka, Y. A., and Saito, H. (2000) Conformational transitions and fibrillation mechanism of human calcitonin as studied by high-resolution solid-state ^{13}C NMR. *Protein Sci. 9*, 867−877.

(8) Naito, A., Kamihira, M., Inoue, R., and Saito, H. (2004) Structural diversity of amyloid fibril formed in human calcitonin as revealed by site-directed ^{13}C solid-state NMR spectroscopy. *Magn. Reson. Chem. 42*, 247−257.

(9) Kamihira, M., Oshiro, Y., Tuzi, S., Nosaka, A. Y., Saito, H., and Naito, A. (2003) Effect of electrostatic interaction on fibril formation of human calcitonin as studied by high resolution solid state ^{13}C NMR. *J. Biol. Chem. 278*, 2859−2865.

(10) Cohen, F. E., and Kelly, J. W. (2003) Therapeutic approaches to protein-misfolding diseases. *Nature 426*, 905−909.

(11) Chimon, S., Shaibat, M. A., Jones, C. R., Calero, D. C., Aizezi, B., and Ishii, Y. (2007) Evidence of fibril-like β-sheet structures in a neurotoxic amyloid intermediate of Alzheimer's β-amyloid. *Nat. Struct. Mol. Biol. 14*, 1157−1164.

(12) Lorenzo, K. M., Razzboni, B., Weir, G. C., and Yankner, B. A. (1994) Pancreatic islet cell toxicity of amylin associated with type-2 diabete mellitus. *Nature 368*, 756−760.

(13) Westermark, P., Engstrom, U., Johnson, K., Westermark, G. T., and Betsholz, C. (1990) Islet amyloid polypeptide: Pinpointing amino acid residues linked to amyloid fibril formation. *Proc. Natl. Acad. Sci. U.S.A. 87*, 5036−5040.

(14) Moriarty, D. F., and Raleigh, D. P. (1999) Effects of sequential proline substitutions on amyloid formation by human amylin20−29. *Biochemistry 38*, 1811−1818.

(15) Tenidis, K., Waldner, M., Bernhagen, J., Fischle, W., Bergmann, M., Weber, M., Merkle, M. L., Voelter, W., Brunner, H., and Kapurniotu, A. (2000) Identification of a penta- and hexapeptide of islet amyloid polypeptide (IAPP) with amyloidogenic and cytotoxic properties. *J. Mol. Biol. 295*, 1055−1071.

(16) Findeis, M. A. (2000) Approaches to discovery and characterization of inhibitors of amyloid β-peptide polymerization. *Biochim. Biophys. Acta 1502*, 76−84.

(17) Gazit, E. (2005) Mechanisms of amyloid fibril self-assembly and inhibition. Model short peptides as a key research tool. *FEBS J. 272*, 5971−5978.

(18) Ono, K., Hamaguchi, T., Naiki, H., and Yamada, M. (2006) Anti-amyloidogenic effects of antioxidants: Implications for the prevention and therapeutics of Alzheimer's disease. *Biochim. Biophys. Acta 1762*, 575−586.

(19) Ono, K., Naiki, H., and Yamada, M. (2006) The development of preventives and therapeutics for Alzheimer's disease that inhibit the formation of β-amyloid fibrils (fAβ), as well as destabilize preformed fAβ. *Curr. Pharm. Des. 12*, 4357−4375.

(20) Naito, A., and Kawamura, I. (2007) Solid-state NMR as a method to reveal structure and membrane-interaction of amyloidogenic proteins and peptides. *Biochim. Biophys. Acta 1768*, 1900−1912.

(21) Levy, M., Porat, Y., Bacharach, E., Shalev, D. E., and Gazit, E. (2008) Phenolsulfonphthalein, but not phenolphthalein, inhibits amyloid fibril formation: Implications for the modulation of amyloid self-assembly. *Biochemistry 47*, 5896−5904.

(22) Porat, Y., Abramowitz, A., Gazit, E., Almeida, M. R., Gales, L., Damas, A. M., Cardoso, I., Saraiva, M. J., Wang, S. S., Chen, Y. T., Chou, S. W., Jaikaran, E. T., Nilsson, M. R., Clark, A., Raghu, P., Reddy, G. B., Sivakumar, B., and Gazit, E. (2006) Inhibition of amyloid fibril formation by polyphenols: Structural similarity and aromatic interactions as a common inhibition mechanism. *Chem. Biol. Drug Des. 67*, 27−37.

(23) Marek, P., Abedini, A., Song, B. B., Knungo, M., Johnson, M. E., Gupta, R., Zaman, W., Wong, S. S., and Raleigh, D. P. (2007) Aromatic interactions are not required for amyloid fibril formation by islet amyloid polypeptide but do influence the rate of fibril formation and fibril morphology. *Biochemistry 46*, 3255−3261.

(24) Shoval, H., Lichtenberg, D., and Gazit, E. (2007) The molecular mechanisms of the anti-amyloid effects of phenols. *Amyloid 14*, 73−87.

(25) Yokozawa, T., Cho, E. J., Hara, Y., and Kitani, K. (2000) Antioxidative activity of green tea treated with radical initiator 2,2′-azobis(2-amidinopropane) dihydrochloride. *J. Agric. Food Chem. 48*, 5068−5073.

(26) Mabe, K., Yamada, M., Oguni, I., and Takahashi, T. (1999) In vitro and in vivo activities of tea catechins against *Helicobacter pylori*. *Antimicrob. Agents Chemother. 43*, 1788−1791.

(27) Uesato, S., Kitagawa, Y., Kamishimoto, M., Kumagai, A., Hori, H., and Nagasawa, H. (2001) Inhibition of green tea catechins against the growth of cancerous human colon and hepatic epithelial cells. *Cancer Lett. 170*, 41−44.

(28) Ono, K., Yoshiike, Y., Takashima, A., Hasegawa, K., Naiki, H., and Yamada, M. (2003) Potent anti-amyloidogenic and fibril-destabilizing effects of polyphenols in vitro: Implications for the prevention and therapeutics of Alzheimer's disease. *J. Neurochem. 87*, 172−181.

(29) Ehrnhoefer, D. E., Bieschke, J., Boeddrich, A., Herbst, M., Masino, L., Lurz, R., Engemann, S., Pastore, A., and Wanker, E. E. (2008) EGCG redirects amyloidogenic polypeptides into unstructured, off-pathway oligomers. *Nat. Struct. Mol. Biol. 15*, 558−566.

(30) Hudson, S. A., Ecroyd, H., Dehle, F. C., Musgrave, I. F., and Carver, J. A. (2009) (−)-Epigallocatechin-3-gallate (EGCG) maintains κ-casein in its pre-fibrillar state without redirecting its aggregation pathway. *J. Mol. Biol. 392*, 689−700.

(31) Bieschke, J., Russ, J., Friedrich, R. P., Ehrnhoefer, D. E., Wobst, H., Neugebauer, K., and Wanker, E. E. (2010) EGCG remodels mature α-synuclein and amyloid-β fibrils and reduces cellular toxicity. *Proc. Natl. Acad. Sci. U.S.A. 107*, 7710−7715.

(32) Meng, F., Abedini, A., Plesner, A., Bruce Verchere, C., and Raleigh, D. P. (2010) The flavanol (−)-epigallocatechin 3-gallate inhibits amyloid formation by islet amyloid polypeptide, disaggregates amyloid fibrils, and protects cultured cells against IAPP-induced toxcity. *Biochemistry 49*, 8127−8133.
(33) Huang, R., Vivekanandan, S., Brender, J. R., Abe, Y., Naito, A., and Ramamoorthy, A. (2012) NMR characterization of monomeric and oligomeric conformations of human calcitonin and its interaction with EGCG. *J. Mol. Biol. 416*, 108−120.
(34) Okahata, Y., Niikura, K., Sugiura, Y., Sawada, M., and Morii, T. (1998) Kinetic studies of sequence-specific binding of GCN4-bZIP peptides to DNA strands immobilized on a 27-MHz quartz-crystal microbalance. *Biochemistry 37*, 5666−5672.
(35) Matsuno, H., Niikura, K., and Okahata, Y. (2001) Design and characterization of asparagine- and lysine-containing alanine-based helical peptides that bind selectively to A-T base pairs of oligonucleotides immobilized on a 27 MHz quartz crystal microbalance. *Biochemistry 40*, 3615−3622.
(36) Matsuno, H., Furusawa, H., and Okahata, Y. (2005) Kinetic studies of DNA cleavage reactions catalyzed by an ATP-dependent deoxyribonuclease on a 27-MHz quartz-crystal microbalance. *Biochemistry 44*, 2262−2270.
(37) Takahashi, S., Matsuno, H., Furusawa, H., and Okahata, Y. (2007) Kinetic analyses of divalent cation-dependent EcoRV digestions on a DNA-immobilized quartz crystal microbalance. *Anal. Biochem. 361*, 210−217.
(38) Okahata, Y., and Ebato, H. (1992) Detection of bioactive compounds using a lipid-coated quartz-crystal microbalance. *Trends Anal. Chem. 11*, 344−354.
(39) Umeyama, M., Kira, A., Nishimura, K., and Naito, A. (2006) Interactions of bovine lactoferricin with acidic phospholipid bilayers and its antimicrobial activity as studied by solid-state NMR. *Biochim. Biophys. Acta 1758*, 1523−1528.
(40) Kamihira, M., Nakazawa, H., Kira, A., Mizutani, Y., Nakamura, M., and Nakayama, T. (2008) Interaction of Tea Catechins with Lipid Bilayers Investigated by a Quartz-Crystal Microbalance Analysis. *Biosci., Biotechnol., Biochem. 72*, 1372−1375.
(41) Okahata, Y., Kawase, M., Niikura, K., Ohtake, F., Furusawa, H., and Ebara, Y. (1998) Kinetic measurements of DNA hybridization on an oligonucleotide-immobilized 27-MHz quartz crystal microbalance. *Anal. Chem. 70*, 1288−1296.
(42) Nakayama, T., Ichiba, M., Kuwabara, M., Kajiya, K., and Kumazawa, S. (2002) Mechanisms and structural specificity of hydrogen peroxide formation during oxidation of catechins. *Food Sci. Technol. Res. 8*, 261−267.
(43) Bae, M. J., Ishii, T., Minoda, K., Kawada, Y., Ichikawa, T., Mori, T., Kamihira, M., and Nakayama, T. (2009) Albumin stabilizes (−)-epigallocatechin gallate in human serum: Binding capacity and antioxidant property. *Mol. Nutr. Food Res. 53*, 709−715.
(44) Jarrett, L. L., and Lansbury, P. T., Jr. (1993) Seeding onedimensional crystallization of amyloid: A pathogenic mechanism in Alzheimer's disease and scrapie? *Cell 73*, 1055−1058.
(45) Wood, S. J., Maleeff, B., Hart, T., and Wetzel, R. (1996) Physical, morphological and functional differences between pH 5.8 and 7.4 aggregates of the Alzheimer's amyloid peptide A*β*. *J. Mol. Biol. 256*, 870−877.
(46) Kajiya, K., Kumazawa, S., and Nakayama, T. (2001) Steric effects on interaction of tea catechins with lipid bilayers. *Biosci., Biotechnol., Biochem. 65*, 2638−2643.